

Domain Knowledge in A*-Based Causal Discovery

Steven Kleineggesse,¹ Andrew R. Lawrence,¹ Hana Chockler^{1,2}

¹ causalens

² Department of Informatics, King's College London
{steven, andrew, hana}@causalens.com

Abstract

Causal discovery has become a vital tool for scientists and practitioners wanting to discover causal relationships from observational data. While most previous approaches to causal discovery have implicitly assumed that no expert domain knowledge is available, practitioners can often provide such domain knowledge from prior experience. Recent work has incorporated domain knowledge into constraint-based causal discovery. The majority of such constraint-based methods, however, assume causal faithfulness, which has been shown to be frequently violated in practice. Consequently, there has been renewed attention towards exact-search score-based causal discovery methods, which do not assume causal faithfulness, such as A*-based methods. However, there has been no consideration of these methods in the context of domain knowledge. In this work, we focus on efficiently integrating several types of domain knowledge into A*-based causal discovery. In doing so, we discuss and explain how domain knowledge can reduce the graph search space and then provide an analysis of the potential computational gains. We support these findings with experiments on synthetic and real data, showing that even small amounts of domain knowledge can dramatically speed up A*-based causal discovery and improve its performance and practicality.

1 Introduction

Discovering causal relationships is of key scientific and practical importance, with wide-ranging applications in molecular biology (Triantafillou et al. 2017), climate science (Ebert-Uphoff and Deng 2014), marketing (Orriols-Puig, Casillas, and Martínez-López 2010) and healthcare (Mani and Cooper 2000), among many others. Interventions or randomized controlled trials are often the most effective and reliable means of identifying causal relationships, but they tend to be challenging, expensive and in some cases unethical. Causal discovery has emerged to tackle this problem by only requiring observational data and has received considerable attention in the recent decades (see Glymour, Zhang, and Spirtes 2019, for a recent review).

Most approaches to causal discovery assume that no prior knowledge about the underlying causal graph is available, meaning that all causal relationships are equally plausible *a priori*. In practice, however, domain experts often have

information about the causal relationships between subsets of variables. They may know from prior experimentation and/or domain expertise that, e.g., two particular variables directly causally influence each other, certain pairs of variables cannot be causally connected, or that there is a causal hierarchy of variables. Incorporating this domain knowledge could dramatically reduce the search space of graphs in causal discovery (Constantinou, Guo, and Kitson 2021).

Recently, Andrews, Spirtes, and Cooper (2020) have proposed a constraint-based causal discovery method that integrates domain knowledge, specifically a hierarchy of nodes, into the search process. Their method, which extends Fast Causal Inference (FCI) (Spirtes, Meek, and Richardson 1995; Zhang 2008), does not assume causal sufficiency, allowing it to detect the presence of latent confounders that are not present in the data. However, being a constraint-based method, the method of Andrews, Spirtes, and Cooper (2020) does assume causal faithfulness, which means that any conditional independencies observed in the data must also be present in the discovered causal graph. This assumption was shown to be frequently violated in practice (Uhler et al. 2013) when the number of observations in the data is limited. Furthermore, causal discovery methods based on FCI can scale exponentially with the number of variables in the data (Glymour, Zhang, and Spirtes 2019) and rely on expensive conditional independence (CI) tests.

There has been renewed interest in score-based causal discovery methods, which, unlike constraint-based approaches, do not rely on CI tests. While the usefulness of these methods has been limited for a long time, mainly due to poor scalability and computational efficiency, recent score-based methods such as FGES (Ramsey et al. 2017), SEGES (Chickering 2020) and A*-based methods (Yuan and Malone 2013; Lu, Zhang, and Yuan 2021; Ng et al. 2021) have been shown to be efficient and scalable even for hundreds of variables. To our knowledge, however, there has been no work that efficiently integrates domain knowledge into score-based causal discovery methods that do not assume causal faithfulness, such as those based on A*.

In this work, we focus on the efficient and sound integration of domain knowledge into A*-based causal discovery algorithms. We believe that our approach improves applicability of score-based causal discovery methods in general and helps to bridge the gap between theoretical approaches

and the needs of practitioners. In summary, the contributions of this work are as follows:

1. Extending A*-based causal discovery methods to efficiently integrate several types of domain knowledge;
2. Providing a theoretical analysis of the computational gains obtained when incorporating domain knowledge;
3. Experimental results demonstrating the computational gains and performance improvements in practice.

2 Background

Let $\mathcal{G} = (\mathbf{V}, \mathbf{E})$ be a directed acyclic graph (DAG) with vertices $\mathbf{V} = \{x_1, \dots, x_d\}$ corresponding to random variables. The set of edges \mathbf{E} contains tuples $(x_i, x_j) \in \mathbf{V}^2$ that specify directed edges going from nodes $x_i \in \text{Pa}_{\mathcal{G}}(x_j)$ to nodes x_j , where $\text{Pa}_{\mathcal{G}}(x_j) \subseteq \mathbf{V} \setminus x_j$ is the parent set of node x_j in \mathcal{G} . The general aim of causal discovery is to use observational data to identify the correct parent set $\text{Pa}_{\mathcal{G}}(x_i)$ for each node x_i , while maintaining acyclicity, thereby fully recovering the true DAG \mathcal{G} .

2.1 Common assumptions in causal discovery

Causal discovery methods typically rely on a set of common assumptions, which we briefly discuss below.

Assumption 1 (Markov). *Consider a DAG \mathcal{G} with vertices \mathbf{V} and a probability distribution \mathbb{P} over the random variables contained in \mathbf{V} . \mathcal{G} and \mathbb{P} satisfy the Markov assumption if and only if every variable $x_i \in \mathbf{V}$ is conditionally independent of its non-descendants $\mathbf{V} \setminus \{\text{descendants}_{\mathcal{G}}(x_i) \cup \text{Pa}_{\mathcal{G}}(x_i) \cup x_i\}$ given its parents $\text{Pa}_{\mathcal{G}}(x_i)$.*

Intuitively, the above Markov assumption says that any conditional independence relationships entailed by the DAG \mathcal{G} also need to be present in the probability distribution \mathbb{P} . There are usually several DAGs that entail the same conditional independence relations, which are therefore known as members of the same Markov equivalence class (MEC). An MEC is uniquely determined by its skeleton and its v-structures (Pearl 2009), i.e. collider connections of the form $X \rightarrow Y \leftarrow Z$ where X and Z are not connected (also known as unshielded colliders). An important type of MEC is a completed partially directed acyclic graph (CPDAG), which contains both undirected and directed edges that define its skeleton and v-structures (Meek 1995).

Assumption 2 (Faithfulness). *Consider a DAG \mathcal{G} with vertices \mathbf{V} and a probability distribution \mathbb{P} over the random variables contained in \mathbf{V} . \mathcal{G} and \mathbb{P} satisfy the Faithfulness assumption if and only if \mathbb{P} does not imply any conditional independence relations that are not already entailed by the Markov assumption.*

The faithfulness assumption above says that any conditional independence relationships entailed by the probability distribution \mathbb{P} also need to be present in the DAG \mathcal{G} , which can be understood as the reverse of the Markov assumption. Due to errors in conditional independence testing, typically occurring due to finite data, this assumption has been shown to often be approximately violated in practice (Uhler et al. 2013).

Assumption 3 (Sufficiency). *A DAG \mathcal{G} satisfies the causal sufficiency assumption if there are no unmeasured common causes.*

The above causal sufficiency assumption intuitively says that all common causes should be captured by the DAG, meaning that there should not be any unknown, or unmeasurable, latent confounders.

2.2 Score-based causal discovery

In general, score-based causal discovery methods optimize a score-function that defines the fit of candidate causal structures, e.g. parent-children combinations, until we obtain a DAG that is optimal with respect to the particular score function used (see Glymour, Zhang, and Spirtes 2019, for a recent review). Commonly-used score functions are the Bayesian information criterion (BIC) or minimum description length (MDL) for continuous data (Schwarz 1978), the BGe score for linear Gaussian data (Geiger and Heckerman 1994) and the BDeu score for discrete data (Heckerman, Geiger, and Chickering 1995).

We follow previous work on A*-based causal discovery (Yuan and Malone 2013; Lu, Zhang, and Yuan 2021; Ng et al. 2021) and utilize the BIC score function, thereby assuming linearity and Gaussianity.

Definition 1 (BIC in Causal Discovery). *Assume that the relationship between a node x_i and its parents $\text{Pa}_{\mathcal{G}}(x_i)$ is modeled by a parametrized function $f_{\theta}(\text{Pa}_{\mathcal{G}}(x_i))$ that is trained in a regression task, where θ are some model parameters. The BIC score for node x_i is given by*

$$S_{\text{BIC}}(x_i) = k \log N - 2 \log L_{\max}, \quad (1)$$

where k is the number of parameters in the functional relationship between parents and children, N is the number of observations in the data and L_{\max} is the value of the maximized likelihood function after training. Under the assumptions of linearity and Gaussianity, the BIC score function can be approximated as follows,

$$S_{\text{BIC}}(x_i) \approx k \log N + N \log R/N, \quad (2)$$

where R is the sum of squared residuals from ordinary least squares regression.

A prominent example of a score-based causal discovery method is greedy equivalence search (GES) (Chickering 2003). While GES works well in practice, it is a greedy method and therefore only guaranteed to converge to a local optimum. Moreover, GES relies on all of the aforementioned assumptions, i.e. the Markov, faithfulness and sufficiency assumptions.

2.3 A*-based algorithms

Recently, score-based causal discovery methods that are based on A* (Hart, Nilsson, and Raphael 1968), which is a shortest path-finding algorithm, have gained traction. A*-based methods are *exact-search* score-based causal discovery algorithms, meaning that they exhaustively explore the graph search space and are assured to converge to a global optimum, unlike GES. While A*-based methods also rely on

the Markov and sufficiency assumptions, they do not rely on the faithfulness assumption. Instead, assuming that the BIC score function is used, exact-search methods can be shown to rely on the weaker sparsest Markov representation (SMR) assumption (Lu, Zhang, and Yuan 2021; Ng et al. 2021).

Assumption 4 (Sparsest Markov Representation). *Consider a DAG \mathcal{G} with vertices \mathbf{V} and a probability distribution \mathbb{P} over the random variables contained in \mathbf{V} . The Markov equivalence class (MEC) of \mathcal{G} is the unique sparsest MEC that satisfies the Markov assumption with \mathbb{P} .*

The above assumption is also referred to as the (unique) frugality assumption and has various desirable properties (Forster et al. 2018). Importantly, it has been shown that causal discovery methods that rely on the faithfulness assumption can perform worse than those that rely on the SMR assumption (Lu, Zhang, and Yuan 2021; Ng et al. 2021).

A*-based causal discovery methods generally work by first constructing a set of parent graphs for each node, as explained below. These are then traversed efficiently using A* in order to find the optimal parent set for each node.

Constructing parent graphs For a given node x_i , the state space of candidate parent sets $\text{Pa}_{\mathcal{G}}(x_i)$ can be represented by a *parent graph*, which we denote by $\mathcal{G}_{Pa}(x_i)$. Concretely, this parent graph is a Hasse diagram, or order graph, consisting of all combinatorial subsets of variables in $\mathbf{V} \setminus x_i$ (see Yuan and Malone 2013). Figure 1 provides an example parent graph for one variable with three potential parents. Parent graphs are constructed in a top-down approach, with the top node being the empty set \emptyset and the bottom node being all other nodes $\mathbf{V} \setminus x_i$. Importantly, each node in the parent graph represents one potential parent set that has a certain score associated with it, measuring its quality as a parent set, as provided by a score-function such as BIC. The cost of a path from the top to the bottom node is simply the sum of the scores from all traversed nodes. In this context, the shortest path in $\mathcal{G}_{Pa}(x_i)$ is the top-to-bottom path with the minimum total cost. Once we have access to the shortest path for each parent graph $\mathcal{G}_{Pa}(x_1), \dots, \mathcal{G}_{Pa}(x_d)$, we can use these to construct a DAG that is optimal by construction (see Yuan and Malone 2013, for more information).

Traversing parent graphs As mentioned above, finding the shortest path for each parent graph allows us to construct an optimal DAG. Yuan and Malone (2013) proposed to use the A* path-finding algorithm to find this shortest path. One of the main advantages of A* is that it uses a heuristic function that estimates the quality of yet unexplored paths, which means that it does not need to explore the whole search space in order to find the optimal solution. Although this has a higher memory-cost, it allows A* to scale up to larger dimensions by reducing the search space. We refer the reader to the work of Yuan and Malone (2013) for more detailed explanations of the regular A*-based causal discovery method.

Variations Various extensions to the above A*-based causal discovery have been proposed, mostly aiming to increase computational efficiency and scalability. The earliest of these extensions was Triplet A* (Lu, Zhang, and Yuan 2021), which runs the above A*-based algorithm on triplets

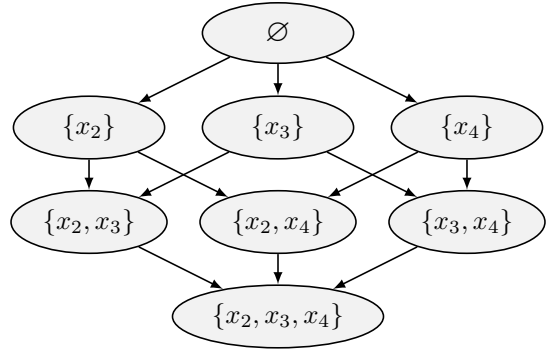


Figure 1: Full parent graph $\mathcal{G}_{Pa}(x_1)$ for node x_1 with potential parents x_2, x_3 and x_4 .

of variables, combines the results and then resolves conflicts between them using a set of rules. However, this extension does not represent an exact-search causal discovery method and, more importantly, it relies on constraint-based approaches, such as PC (Spirtes, Glymour, and Scheines 1993) or MMMB (Tsamardinos, Aliferis, and Statnikov 2003), to identify appropriate triplets, thereby assuming faithfulness. These limitations were rectified by Ng et al. (2021), who proposed A*-SuperStructure and Local A*. Both of these variations rely on a so-called *super-structure*, which is an undirected graph that is a super-set of the skeleton of the true DAG, i.e. the true skeleton with some spurious edges. Ng et al. (2021) use graphical LASSO (Friedman, Hastie, and Tibshirani 2008) to estimate this super-structure and show that this estimation method relies on assumptions strictly weaker than faithfulness. Importantly, the super-structure, often represented by a binary adjacency matrix, specifies forbidden causal relationships which can be used to prune the parent graphs and reduce the search space accordingly. Local A* further improves scalability by looping through local clusters of nodes, as defined by the super-structure, and then applying A*-SuperStructure to each of them, combining the results and resolving any conflicts using a set of rules.

3 Methodology

We define different types of domain knowledge and discuss how to integrate these efficiently with A*-based causal discovery methods. We then provide a theoretical analysis of the potential computational gains obtained.

3.1 Domain knowledge

Many approaches to causal discovery assume that all potential causal structures are equally likely *a priori* (e.g. Chickering 2003; Yuan and Malone 2013; Lu, Zhang, and Yuan 2021). In practice, however, domain experts typically have useful prior experience that they can leverage to formulate domain knowledge about certain causal relationships. It may then be beneficial to integrate this domain knowledge into the causal discovery procedure in order to improve computational efficiency and accuracy. For instance, it is generally accepted that a person's age is a causal driver of their physical height, and not the other way around.

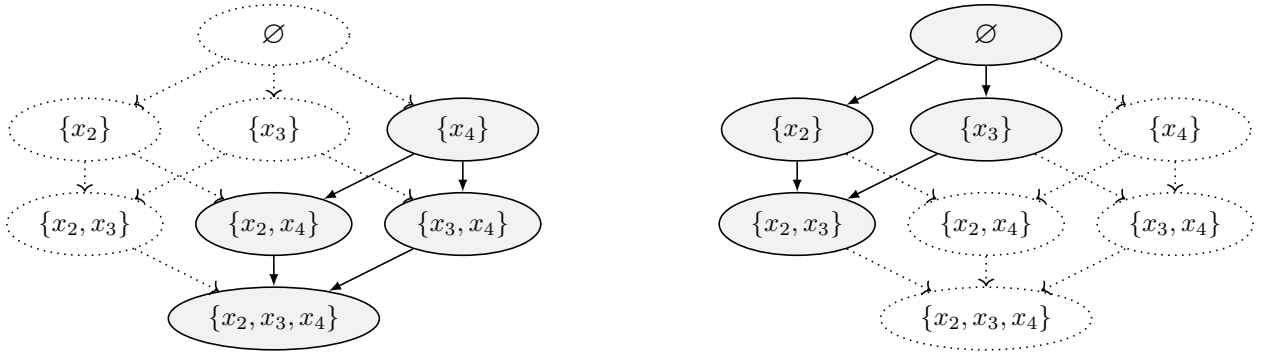


Figure 2: Pruned parent graph $\mathcal{G}_{Pa}(x_1)$ for variable x_1 with potential parents x_2, x_3 and x_4 when incorporating a known edge $x_4 \rightarrow x_1$ (left) and when incorporating a forbidden edge between x_1 and x_4 (right).

There are several ways that domain knowledge can be expressed and, conversely, encoded to be useful in causal discovery (Constantinou, Guo, and Kitson 2021). In this work we focus on the following three common ways:

Definition 2 (Known edges). Domain knowledge that encodes a known, directed edge $x_i \rightarrow x_j$ between two variables $x_i, x_j \in \mathbf{V}$ implies that x_i is most definitely a member of the parent set of x_j , i.e. $x_i \in Pa_{\mathcal{G}}(x_j)$.

Definition 3 (Forbidden edges). Domain knowledge that encodes a forbidden edge between two variables $x_i, x_j \in \mathbf{V}$ implies that neither x_i nor x_j can be a member of each other’s parent set, i.e. $x_i \notin Pa_{\mathcal{G}}(x_j)$ and $x_j \notin Pa_{\mathcal{G}}(x_i)$.

Definition 4 (Tiers). Domain knowledge that encodes tiers $\mathbf{T} = \{\mathbf{T}_1, \dots, \mathbf{T}_n\}$ specifies a causal hierarchy of variables, which states that variables in later tiers, e.g., \mathbf{T}_n , cannot be causal drivers of variables in earlier tiers, e.g., \mathbf{T}_1 . Specifically, if variable x_i is a member of \mathbf{T}_k , variable x_j is a member of \mathbf{T}_s and $k < s$, the domain knowledge indicates that x_i may be a parent of x_j , but x_j cannot be a parent of x_i . If x_i and x_j are in the same tier, i.e. $k = s$, then either variable may be a parent of the other.

Meek (1995) was among the first to consider domain knowledge that contains known edges and forbidden edges in constraint-based causal discovery. Similarly, Scheines et al. (1998) were the first to insert tiered domain knowledge into constraint-based causal discovery. More recently, Andrews, Spirtes, and Cooper (2020) inserted tiered domain knowledge into the popular FCI (Spirtes, Meek, and Richardson 1995; Zhang 2008) constraint-based algorithm. To our knowledge, however, the above ways of encoding domain knowledge have not been used in conjunction with exact-search score-based causal discovery methods.

We here make a few assumptions about the provided domain knowledge. First, we assume that there is *no conflicting domain knowledge*, i.e. we cannot specify a known edge $x_i \rightarrow x_j$ when we have already specified a forbidden edge between both variables. Second, we assume that the *domain knowledge is correct*, i.e. that any relationships encoded in the domain knowledge are also present in the ground-truth. Third, we assume that known and forbidden edges are examples of *hard* domain knowledge, i.e. the encoded domain

knowledge needs to be present in the output of the algorithm. Tiers, on the other hand, is a mixture of *soft and hard* domain knowledge, since variables in earlier tiers can potentially be parents of those in later tiers (soft), but those in later tiers cannot be parents of those in earlier tiers (hard).

3.2 Integrating domain knowledge with A^*

Previous exact-search score-based causal discovery methods that could not leverage domain knowledge have had to explore the entire graph search space. By effectively integrating domain knowledge, however, we are able to constrain this search space and, therefore, speed up causal discovery. In this work we are concerned with A^* -based causal discovery, which mainly consists of two steps: 1) constructing the parent graphs, including computing all relevant scores, and 2) traversing these parent graphs using A^* to find shortest paths, which can then be combined to yield optimal parent sets. Below, we discuss how integration of the aforementioned types of domain knowledge affects each step.

Pruning of the parent graphs As explained previously, parent graphs are ordered graphs of all potential parent sets, as shown in Figure 1. Let us now assume that we are provided with some domain knowledge that is in direct violation with some of these potential parent sets. Since we are assuming that our domain knowledge is correct, we can prune away those potential parent sets that are causing the violation, only leaving parent sets that are allowed by the provided domain knowledge. Consequently, we do not need to perform expensive score function evaluations for those potential parent sets that have been pruned away, which can result in significant computational gains.

In this work, we consider several different types of domain knowledge, specifically known edges, forbidden edges and tiers. First, consider the case of incorporating a known edge $x_i \rightarrow x_j$ into the causal discovery process. By definition, x_i has to be included in the parent set of x_j , which means that the parent graph $\mathcal{G}_{Pa}(x_j)$ can be pruned in such a way that it only contains parent sets that incorporate x_i . Conversely, the optimal parent set of x_i cannot include x_j and, therefore, all potential parent sets in the parent graph $\mathcal{G}_{Pa}(x_i)$ that contain x_j can be pruned away. We visualize this process in the left of Figure 2 for a small parent graph.

Next, consider the case of incorporating a forbidden edge between two variables x_i and x_j , implying that neither of them can be in the parent set of the other. Similar to before, we can prune away all potential parent sets in their parent graphs that contain the other variable, such that no parent sets in $\mathcal{G}_{Pa}(x_i)$ contain x_j , and vice versa. This process is visualized for a small parent graph in the right of Figure 2.

Lastly, let us consider domain knowledge that includes tiers, i.e. a hierarchy of variables. This type of domain knowledge specifies that variables in tier \mathbf{T}_k may be parents of variables in \mathbf{T}_s , for $k < s$, but members in \mathbf{T}_s cannot be parents of members in \mathbf{T}_k . Therefore, assuming that a variable x_i is in tier \mathbf{T}_k , we can prune its parent graph $\mathcal{G}_{Pa}(x_i)$ such that no potential parent sets contain any members in later tiers $\mathbf{T}_{>k}$. We here focus on the common and practical scenario of having one source variable and one sink variable. This results in three tiers: 1) a source variable, 2) all other variables and 3) a sink variable. In this setting, the parent graph of the source variable can be pruned such that it only contains the empty set \emptyset . Similarly, the parent graphs of all variables besides the source and sink variables can be pruned such that they do not include the sink variable. See the supplementary materials for more information on the general case of arbitrary tiers.

Faster shortest-path finding Using domain knowledge to prune parent graphs in A^* -based causal discovery, as explained above, directly reduces the number of necessary score function evaluations. In addition, pruning parent graphs further allows us to reduce the number of possible paths from the top node to the bottom node in the parent graph. This implies an important speed-up during the second step of A^* -based methods, which is concerned with finding the shortest-path from the top to bottom node using the A^* algorithm. Unfortunately, it is difficult to estimate the impact of reducing the number of potential paths, due to the heuristic function that A^* uses to limit the search space. Furthermore, A^* may ignore entire parts of the parent graph if it notices that the scores become worse as it gets towards the bottom node (see Yuan and Malone 2013). This may result in the bottom node not being the final node during the shortest path-finding, further complicating an analysis of how domain knowledge exactly impacts this procedure. Nonetheless, this operation reduces the path-finding search space in the worst-case scenario and could therefore have a significant impact, especially for a large number of variables where the space of possible paths is exponentially large. As an example, consider the parent graph in Figure 1 and let us insert a known edge, as done in Figure 2, which results in a reduction of the number of top-to-bottom paths from 6 to 2.

Applying Meek’s rules A^* -based causal discovery algorithms are generally only guaranteed to recover the true completed partially directed acyclic graph (CPDAG) (see Ng et al. 2021), which represents the Markov equivalence class (MEC) of the underlying true DAG. Often, this CPDAG is computed directly from a DAG estimate that is obtained after running A^* -based causal discovery (as in Ng et al. 2021). While the original DAG estimate may be consistent with the provided domain knowledge, this may not be

true for the corresponding CPDAG. As such, we here propose to apply the common rule set of Meek (1995) to insert the provided domain knowledge into the CPDAG obtained from A^* -based causal discovery. Consequently, this *modified CPDAG* no longer represents the MEC of the true DAG.

3.3 Computational gains

We have previously explained how the number of score function evaluations can be reduced by pruning the parent graphs according to the domain knowledge. The exact number of final score function evaluations, however, is difficult to predict for any combination of domain knowledge. Nonetheless, for certain types of domain knowledge it is possible to provide estimates of the computational gains by deriving the exact reduction in score function evaluations. Additionally, the pruned parent graphs also result in a potentially faster executing of the A^* shortest-path finding algorithm, since fewer paths need to be searched. Quantifying the complexity of this operation, and the corresponding gains, is difficult due to the heuristic function in A^* (Lu, Zhang, and Yuan 2021; Ng et al. 2021), which is why we focus on the reduction in score function evaluations to provide us with an estimate of the overall computational gains. In the interest of space, proofs of the following lemmas and theorems appear in the supplementary material.

We here only consider regular A^* and not the variations A^* -SuperStructure or Local A^* , since these rely on a super-structure that also results in a pruning of the parent graphs. Because estimation of this super-structure is data-driven, it is not possible to predict the extent of this pruning and its interaction with the pruning resulting from domain knowledge. We note, however, that A^* is a special worst-case scenario of A^* -SuperStructure and Local A^* (Ng et al. 2021).

First, we quantify the number of score function evaluations in the worst-case scenario of regular A^* -based causal discovery by means of the following lemma.

Lemma 1. *A full parent graph \mathcal{G}_{PA} has $2^{(p-1)}$ nodes, each representing a different potential parent set. Given a data set containing p variables, A^* -based causal discovery requires $p2^{(p-1)}$ score function evaluations in the worst case.*

Let us then consider the case of incorporating known, directed edges into A^* -based causal discovery. Theorem 2 provides an estimate of the computational gains when incorporating one known, directed edge.

Theorem 2. *Given a set of full parent graphs, incorporating the domain knowledge of one directed edge reduces the maximum number of score function computations in regular A^* -based causal discovery from $p2^{p-1}$ to $(p-1)2^{p-1}$, where p is the total number of nodes.*

Next, we consider incorporating a forbidden edge into A^* -based causal discovery, with Theorem 3 providing an estimate of the corresponding computational gains.

Theorem 3. *Given a set of full parent graphs, incorporating the domain knowledge of one forbidden edge reduces the maximum number of score function computations in regular A^* -based causal discovery from $p2^{p-1}$ to $(p-1)2^{p-1}$, where p is the total number of nodes.*

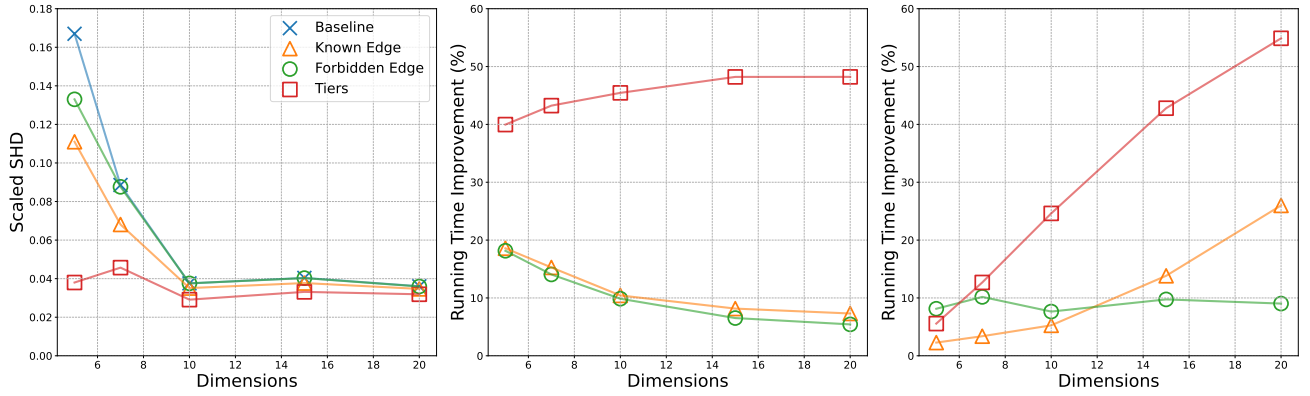


Figure 3: Results for applying A*-based causal discovery on the synthetic data set when incorporating different types of domain knowledge. *Left*: Performance improvements as measured by the scaled SHD (lower is better) for varying dimensions, averaged over 100 repeats. *Middle*: Percentage improvement in running times of regular A* (middle) for varying dimensions, as compared to not incorporating any domain knowledge, averaged over 100 repeats. *Right*: Percentage improvement in running times of A*-SuperStructure for varying dimensions, as compared to not incorporating any domain knowledge, averaged over 100 repeats.

Interestingly, this estimate of the computational gains for incorporating a forbidden edge is exactly the same as that for incorporating a known edge. This may provide useful advice for practitioners since, in the age of big data, causal graphs in practice tend to be sparse. A domain expert may, therefore, find it easier to specify a forbidden edge than a known edge. Since both cases yield the same computational gains, domain experts may therefore want to first focus on specifying as many forbidden relationships as possible.

Lastly, we consider the case of incorporating tiered domain knowledge into A*-based causal discovery. As mentioned before, we here focus on the common and practical case of having one source node and one sink node, ultimately resulting in three tiers. Theorem 4 provides an estimate of the ensued computational gains (see the supplementary material for a theorem with tiers of arbitrary sizes).

Theorem 4. *Given a set of full parent graphs, incorporating tiered domain knowledge that includes exactly one source variable and one sink variable, resulting in three tiers, halves the maximum number of score function computations in regular A*-based causal discovery.*

The above theorem implies that the potential computational gains from incorporating tiered domain knowledge far outweigh those from incorporating known or forbidden edges, especially when the underlying causal graph is large. Theorem 4 therefore suggests that specifying tiered domain knowledge should be a priority for practitioners.

4 Experiments

In this section we provide experimental results of the computational gains obtained when integrating several types of domain knowledge with A*-based causal discovery methods. We first consider synthetic data that has been generated using randomly-sampled DAGs. We then study the application of our approach on the commonly-used, real Sachs data set (Sachs et al. 2005). See the supplementary material for more detailed explanations of the experimental setup.

4.1 Evaluation

We evaluate the performance of all causal discovery methods by their ability to recover the true graph, as measured by the structural hamming distance (SHD) between *modified* CPDAGs. Where applicable, we also scale the SHD by the number of possible edges $p(p-1)/2$. Lastly, we also assess all methods by their computational running time.

4.2 Synthetic Data

We here consider synthetic data that has been generated using a linear structural equation model (SEM) with Gaussian noise and a randomly-sampled Erdős-Rényi graph. For all synthetic data experiments, we sample ground-truth DAGs with an average degree of 2 and varying dimensions of $p \in \{5, 7, 10, 15, 20\}$. For each DAG, we use a linear SEM with randomly-sampled parameters to generate 500 observations. Throughout our experiments, known edges are randomly sampled from the set of true edges, whereas forbidden edges are randomly sampled from its complement set. Similarly, the source and sink node for the tiers domain knowledge are randomly sampled from the set of true source and sink nodes, respectively.

Results Figure 3 summarizes the performance and computational gains obtained when integrating different types of domain knowledge with A*-based causal discovery. The left figure shows the scaled SHD as a function of data dimensions for regular A*-based causal discovery. While all approaches result in smaller scaled SHD for increasing dimensions, it is apparent that integrating domain knowledge can largely reduce the SHD across all dimensions. The effect of incorporating tiers appears to be the highest, followed by that of incorporating known edges and then, lastly, that of incorporating forbidden edges. Using Student’s t-tests, we are able to ascertain that the SHD improvements for tiers and known edges are, in fact, statistically significant with a p-value threshold of 0.05, while those for forbidden edges are not (see the supplementary material for more information).

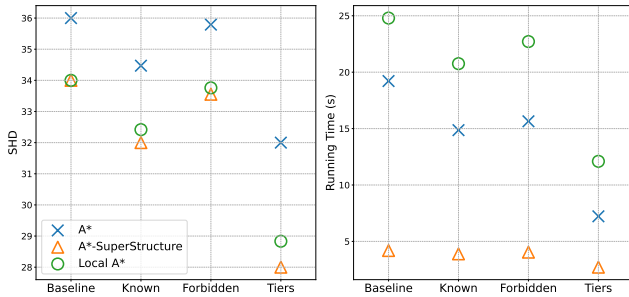


Figure 4: Results for applying A*-based causal discovery on the Sachs data set for different types of domain knowledge.

Next, we turn towards percentage improvements in the running time of A*-based causal discovery, as shown in the middle and right of Figure 3. The middle plot shows how incorporating different types of domain knowledge can help speed up regular A*. The computational gains for incorporating known edges and for incorporating forbidden edges fall off inversely proportional to the data dimensionality, which is entirely in line with our theoretical analysis in the methodology section, i.e. Theorems 2 and 3. For tiers, the percentage improvement starts off at around 40% and then increases to 50% at 15 and 20 dimensions, which matches the gain predicted by Theorem 4. While there is a slight mismatch for small dimensions, the corresponding confidence intervals (see the supplementary material) confidently capture the expected gain.

Similarly, the right plot in Figure 3 shows how incorporating domain knowledge can help speed up A*-SuperStructure (we show a similar plot for Local A* in the supplementary material). Interestingly, the behavior for A*-SuperStructure appears largely different to that of regular A*. Here, the computational gains for incorporating known edges and incorporating tiers grow nearly linearly with the dimensions, whereas the running time improvements for incorporating forbidden edges stay roughly constant. Recall that A*-SuperStructure has a data-driven skeleton-estimation step which can have large computational overhead. In fact, this overhead may be the computational bottleneck of A*-SuperStructure at small dimensions, as can be seen when looking at absolute running times as a function of dimensions (see the supplementary material). While integrating domain knowledge helps in reducing the number of score function evaluations, it does not help with the data-driven estimation of the super structure in A*-SuperStructure. Moreover, as noted previously, Theorems 2–4 are only valid for regular A*-based causal discovery, because of the unclear interaction of the super-structure induced parent graph pruning and the domain knowledge induced pruning.

4.3 Sachs Data

We here consider the real protein signalling data set of Sachs et al. (2005), which describes protein interactions in human cells. The data set contains 11 continuous variables with 7,466 observations and, importantly, has a known ground-truth DAG that was formed by experts with the help of inter-

ventional data (see the supplementary material).

Similar to before, we are concerned with analyzing the impact of integrating different types of domain knowledge with A*-based causal discovery, specifically that of known edges, forbidden edges and tiers. To this end, we first generate all possible combinations of such domain knowledge, as given by the known ground-truth. For incorporating known edges, this implies running A*-based causal discovery for every possible edge that could be inserted (17 in total). Similarly, for incorporating forbidden edges, this means running causal discovery for all non-edges (of which there are 38). There are 2 source variables and 4 sink variables in the ground-truth DAG, resulting in 8 different sets of tiers.

In Figure 4 we summarize the results of integrating these sets of domain knowledge with regular A*, A*-SuperStructure and Local A*. The left plot shows how the SHD is affected by considering different types of domain knowledge and different A*-based methods. All types of domain knowledge generally improve SHD, with tiers having the largest impact, followed by known edges and then forbidden edges, which is similar to results of the synthetic data set experiments. Notably, A*-SuperStructure appears to be affected most by the insertion of domain knowledge and also results in the largest SHD improvements. Even though both A*-SuperStructure and Local A* rely on graphical LASSO to compute a super-structure, the latter does not seem to be affected as much as the former.

Finally, the right plot in Figure 4 shows absolute running times for A*-based causal discovery when incorporating different types of domain knowledge. Regular A* seems to be affected the most by the insertion of domain knowledge, whereas A*-SuperStructure does not seem to be affected much at all. One of the reasons for this observation may be the potentially large overhead due to the super-structure computation, which was already observed for relatively small synthetic data sets (see Figure 4). While Local A* appears to be the slowest method, we note that this method has the potential to be parallelized over several CPUs (Ng et al. 2021). Overall, every method appears to be positively affected by domain knowledge, with respect to both SHD and running time.

5 Conclusions

In this work we provided a sound method for integrating different types of domain knowledge with A*-based causal discovery methods. In doing so, we discussed how domain knowledge can affect each step of the causal discovery process and offered a theoretical analysis of the potential computational gains, as measured by a reduction in the number of score function computations. We supported our findings with synthetic and real data, finding that domain knowledge can help improve recovery of the ground-truth and computational running time in nearly every setting. Furthermore, we showed that various extensions, such as A*-SuperStructure and Local A*, can show significantly different responses to the integration of domain knowledge than regular A*.

One of the current main limitations of A*-based causal discovery is that it is only guaranteed to converge to the global optimum in the linear and Gaussian setting. In the

future, it may be interesting to investigate, theoretically and empirically, how the integration of domain knowledge affects the non-linear and non-Gaussian setting, perhaps even considering discrete data.

References

- Andrews, B.; Spirtes, P.; and Cooper, G. F. 2020. On the Completeness of Causal Discovery in the Presence of Latent Confounding with Tiered Background Knowledge. In *Proceedings of the Twenty Third International Conference on Artificial Intelligence and Statistics*, volume 108 of *Proceedings of Machine Learning Research*, 4002–4011. PMLR.
- Chickering, D. M. 2003. Optimal Structure Identification with Greedy Search. *J. Mach. Learn. Res.*, 3(0): 507–554.
- Chickering, D. M. 2020. Statistically Efficient Greedy Equivalence Search. In *Proceedings of the 36th Conference on Uncertainty in Artificial Intelligence (UAI)*, volume 124 of *Proceedings of Machine Learning Research*, 241–249. PMLR.
- Constantinou, A. C.; Guo, Z.; and Kitson, N. K. 2021. The impact of prior knowledge on causal structure learning. *arXiv e-prints*, arXiv:2102.00473.
- Ebert-Uphoff, I.; and Deng, Y. 2014. Causal Discovery from Spatio-Temporal Data with Applications to Climate Science. In *13th International Conference on Machine Learning and Applications*, 606–613.
- Forster, M.; Raskutti, G.; Stern, R.; and Weinberger, N. 2018. The Frugal Inference of Causal Relations. *The British Journal for the Philosophy of Science*, 69(3): 821–848.
- Friedman, J. H.; Hastie, T. J.; and Tibshirani, R. 2008. Sparse inverse covariance estimation with the graphical lasso. *Biostatistics*, 9(3): 432–41.
- Geiger, D.; and Heckerman, D. 1994. Learning Gaussian Networks. In *UAI’94*.
- Glymour, C.; Zhang, K.; and Spirtes, P. 2019. Review of Causal Discovery Methods Based on Graphical Models. *Frontiers in Genetics*, 10.
- Hart, P. E.; Nilsson, N. J.; and Raphael, B. 1968. A Formal Basis for the Heuristic Determination of Minimum Cost Paths. *IEEE Transactions on Systems Science and Cybernetics*, 4(2): 100–107.
- Heckerman, D.; Geiger, D.; and Chickering, D. 1995. Learning Bayesian Networks: The Combination of Knowledge and Statistical Data. *Machine Learning*, 20: 197–243.
- Lu, N. Y.; Zhang, K.; and Yuan, C. 2021. Improving Causal Discovery By Optimal Bayesian Network Learning. *Proceedings of the AAAI Conference on Artificial Intelligence*, 35(10): 8741–8748.
- Mani, S.; and Cooper, G. F. 2000. Causal discovery from medical textual data. *Proceedings. AMIA Symposium*, 542–6.
- Meek, C. 1995. Causal Inference and Causal Explanation with Background Knowledge. In *Proceedings of the Eleventh Conference on Uncertainty in Artificial Intelligence*, UAI’95, 403–410.
- Ng, I.; Zheng, Y.; Zhang, J.; and Zhang, K. 2021. Reliable Causal Discovery with Improved Exact Search and Weaker Assumptions. In *NeurIPS 2021*.
- Orriols-Puig, A.; Casillas, J.; and Martínez-López, F. J. 2010. Automatic Discovery of Potential Causal Structures in Marketing Databases Based on Fuzzy Association Rules. In *Marketing Intelligent Systems Using Soft Computing: Managerial and Research Applications*, 181–206. Springer Berlin Heidelberg.
- Pearl, J. 2009. *Causality*. Cambridge University Press, 2 edition.
- Ramsey, J.; Glymour, M.; Sanchez-Romero, R.; and Glymour, C. 2017. A million variables and more: the Fast Greedy Equivalence Search algorithm for learning high-dimensional graphical causal models, with an application to functional magnetic resonance images. *International Journal of Data Science and Analytics*, 3.
- Sachs, K.; Perez, O.; Pe’er, D.; Lauffenburger, D. A.; and Nolan, G. P. 2005. Causal Protein-Signaling Networks Derived from Multiparameter Single-Cell Data. *Science*, 308(5721): 523–529.
- Scheines, R.; Spirtes, P. L.; Glymour, C.; Meek, C.; and Richardson, T. S. 1998. The TETRAD Project: Constraint Based Aids to Causal Model Specification. *Multivariate behavioral research*, 33 1: 65–117.
- Schwarz, G. 1978. Estimating the Dimension of a Model. *The Annals of Statistics*, 6(2): 461 – 464.
- Spirtes, P.; Glymour, C.; and Scheines, R. 1993. *Causation, Prediction and Search*. Springer-Verlag.
- Spirtes, P.; Meek, C.; and Richardson, T. 1995. Causal Inference in the Presence of Latent Variables and Selection Bias. In *Proceedings of the Eleventh Conference on Uncertainty in Artificial Intelligence*, UAI’95, 499–506.
- Triantafyllou, S.; Lagani, V.; Heinze-Deml, C.; Schmidt, A.; Tegner, J.; and Tsamardinos, I. 2017. Predicting Causal Relationships from Biological Data: Applying Automated Causal Discovery on Mass Cytometry Data of Human Immune Cells. *Scientific Reports*, 7.
- Tsamardinos, I.; Aliferis, C. F.; and Statnikov, A. 2003. Time and Sample Efficient Discovery of Markov Blankets and Direct Causal Relations. In *Proceedings of the Ninth ACM SIGKDD International Conference on Knowledge Discovery and Data Mining*, KDD ’03, 673–678.
- Uhler, C.; Raskutti, G.; Bühlmann, P.; and Yu, B. 2013. Geometry of the faithfulness assumption in causal inference. *The Annals of Statistics*, 41(2): 436 – 463.
- Yuan, C.; and Malone, B. 2013. Learning Optimal Bayesian Networks: A Shortest Path Perspective. *J. Artif. Int. Res.*, 48(1): 23–65.
- Zhang, J. 2008. On the completeness of orientation rules for causal discovery in the presence of latent confounders and selection bias. *Artificial Intelligence*, 172(16): 1873–1896.

Technical Appendix for Domain Knowledge in A*-Based Causal Discovery

A Additional theoretical contributions

A.1 Score computations in a full parent graph

Lemma 5. *A full parent graph \mathcal{G}_{PA} has $2^{(p-1)}$ nodes, each representing a different potential parent set. Given a data set containing p variables, A*-based causal discovery requires $p2^{(p-1)}$ score function evaluations in the worst case.*

Proof. Consider a set of p variables $X = \{x_1, \dots, x_p\}$ and the full parent graph $\mathcal{G}_{PA}(x_i)$ of variable x_i , which is an ordered graph of all potential parent sets of x_i in a causal graph. Let us define a level l within the parent graph where each potential parent set has exactly l elements. By definition, the full parent graph $\mathcal{G}_{PA}(x_i)$ contains potential parent sets with an increasing number of elements, starting from the empty set \emptyset (top level) to all other variables $X \setminus x_i$ (bottom level), which means that $\mathcal{G}_{PA}(x_i)$ contains p levels $l \in \{0, \dots, p-1\}$. In order to find out how many potential parent sets correspond to each level l , we need to count how many potential parent sets can be chosen from $X \setminus x_i$ such that they contain l elements. This number can be obtained exactly by applying the choose operator $C(p-1, l)$. We can then compute how many nodes a full parent graph $\mathcal{G}_{PA}(x_i)$ contains by summing over all levels l , i.e.

$$|\mathcal{G}_{PA}(x_i)| = \sum_{l=0}^{p-1} C(p-1, l) = 2^{p-1}, \quad (3)$$

where the second step is a direct consequence of the well-known binomial theorem. Since we have p of such full parent graphs, the number of score function evaluations in A*-based causal discovery is precisely $p2^{p-1}$. \square

A.2 Computational gains for known edges

Theorem 6. *Given a set of full parent graphs, incorporating the domain knowledge of one directed edge reduces the maximum number of score function computations in regular A*-based causal discovery from $p2^{p-1}$ to $(p-1)2^{p-1}$, where p is the total number of nodes.*

Proof. Let us insert a known edge from variable x_i to variable x_j , where $i, j \in \{1, \dots, p\}$ and $i \neq j$. Since x_i is assured to be a parent of x_j , we do not need to compute scores for nodes, i.e. potential parent sets, in the parent graph of x_i and x_j that violate this known causal relationship.

First, consider the full parent graph $\mathcal{G}_{PA}(x_i)$ of x_i . By incorporating the domain knowledge that $x_i \rightarrow x_j$, we know that x_j cannot be a parent of x_i and, therefore, we can remove all nodes in the parent graph of x_i that contain x_j . This changes the number of potential parents of x_i from $p-1$ to $p-2$, which, according to Lemma 5, reduces the number of score computations in this parent graph from 2^{p-1} to 2^{p-2} .

Second, consider the parent graph $\mathcal{G}_{PA}(x_j)$ of x_j in a similar manner. By incorporating the domain knowledge that $x_i \rightarrow x_j$, we know that x_i has to be in the optimal parent set of x_j . This means that we can prune all nodes in this parent

graph that do not contain x_i . In order to deduce the reduction in score computations, recall from Lemma 5 that the number of nodes in the full parent graph $\mathcal{G}_{PA}(x_j)$, without incorporating domain knowledge, is given by

$$|\mathcal{G}_{PA}(x_j)| = \sum_{l=0}^{p-1} C(p-1, l) = 2^{p-1}, \quad (4)$$

where $C(p-1, l)$ denotes the number of combinations that we can choose l parents out of $p-1$ potential parents. Incorporating the known edge $x_i \rightarrow x_j$ implies that the parent set of x_j cannot be empty, which means that the $l=0$ term can be dropped from the above sum. Furthermore, since x_i is a required parent it needs to be included in every potential parent set, which means that we only need to choose $l-1$ other parents from a total pool of $p-2$ parents for every term in the above sum. The variable x_i can then simply be added to every chosen parent set to construct a valid parent set. The number of score computations for this pruned parent graph $\mathcal{G}_{PA}(x_j)$ is therefore given by

$$|\mathcal{G}_{PA}(x_j)| = \sum_{l=1}^{p-1} C(p-2, l-1) \quad (5)$$

$$= \sum_{l'=1}^{p-2} C(p-2, l') \quad (6)$$

$$= 2^{p-2}, \quad (7)$$

where made a change of variables $l' = l-1$ in the second line and applied Lemma 5 in the third line.

Therefore, the total number of score function evaluations across all pruned parent graphs is

$$2^{p-2} + (p-2)2^{p-1} + 2^{p-2} = (p-1)2^{p-1}, \quad (8)$$

where the first and third term are due to the parent graphs of x_i and x_j , respectively, and the second term is due to the parent graphs of all the other nodes $X \setminus \{x_i, x_j\}$, which remain unchanged. \square

A.3 Computational gains for forbidden edges

Theorem 7. *Given a set of full parent graphs, incorporating the domain knowledge of one forbidden edge reduces the maximum number of score function computations in regular A*-based causal discovery from $p2^{p-1}$ to $(p-1)2^{p-1}$, where p is the total number of nodes.*

Proof. Let us insert a forbidden edge between variable x_i and variable x_j , where $i, j \in \{1, \dots, p\}$ and $i \neq j$. Since neither variable can be in the parent set of the other variable, we do not need to compute scores for nodes, i.e. potential parent sets, in the parent graph of x_i and x_j that violate this known causal relationship.

First, consider the full parent graph $\mathcal{G}_{PA}(x_i)$ of x_i . Since we know that x_j cannot be a parent of x_i , we can remove all nodes in the parent graph of x_i that contain x_j . This

changes the number of potential parents of x_i from $p - 1$ to $p - 2$, which, according to Lemma 5, reduces the number of score computations in this parent graph from 2^{p-1} to 2^{p-2} . The exact same argument then applies to the parent graph $\mathcal{G}_{Pa}(x_j)$ of x_j , which can be pruned such that it does not contain any potential parent sets that involve x_i . This similarly reduces the number of score computations from 2^{p-1} to 2^{p-2} .

Therefore, the total number of score function evaluations across all pruned parent graphs is

$$2^{p-2} + (p - 2)2^{p-1} + 2^{p-2} = (p - 1)2^{p-1}, \quad (9)$$

where the first and third term are due to the parent graphs of x_i and x_j , respectively, and the second term is due to the parent graphs of all the other nodes $X \setminus \{x_i, x_j\}$, which remain unchanged. \square

A.4 Computational gains for tiers with one source and one sink variable

Theorem 8. *Given a set of full parent graphs, incorporating tiered domain knowledge that includes exactly one source variable and one sink variable, resulting in three tiers, halves the maximum number of score function computations in regular A^* -based causal discovery.*

Proof. Consider the tiered domain knowledge $\mathbf{T} = \{\mathbf{T}_1, \mathbf{T}_2, \mathbf{T}_3\}$, where $\mathbf{T}_1 = \{x_i\}$ contains a single source variable x_i , $\mathbf{T}_3 = \{x_j\}$ contains a single sink variable x_j and $\mathbf{T}_2 = \{x_1, \dots, x_p\} \setminus \{x_i, x_j\}$ consists of all other variable except the source and sink variables. Here, the tiers \mathbf{T} specifies that directed edges can never go from elements in \mathbf{T}_3 to elements in either \mathbf{T}_1 or \mathbf{T}_2 , or from elements in \mathbf{T}_2 to elements in \mathbf{T}_1 . We can deduce the reduction in the maximum number of score function computations by pruning the set of parent graphs such that they conform with \mathbf{T} .

Consider the full parent graph $\mathcal{G}_{Pa}(x_i)$ of the source variable x_i . Since x_i is contained in the first tier \mathbf{T}_1 , the domain knowledge specifies that it has no parents and therefore we do not need to perform any score computations in its parent graph at all. In contrast, the full parent graph $\mathcal{G}_{Pa}(x_j)$ of the sink variable x_j remains unchanged, since it is contained in the last tier \mathbf{T}_3 , which means that its maximum number of score computations is still 2^{p-1} .

Let us now consider the full parent graph $\mathcal{G}_{Pa}(x_k)$ of any variable $x_k \in \mathbf{T}_2$. Since there cannot be directed edges from the sink variable $x_j \in \mathbf{T}_3$ to x_k , we need to prune all nodes in the full parent graph that contain the variable x_j . This reduces the number of potential parents from $p - 1$ to $p - 2$, which, according to Lemma 5, means that the parent graph of x_k has 2^{p-2} nodes. Since there are $p - 2$ variables in the second tier \mathbf{T}_2 , this results in a maximum of $(p - 2)2^{p-2}$ score computations.

Adding the number of score computations for all full parent graphs yields $(p - 2)2^{p-2} + 2^{p-1} = \frac{p}{2}2^{p-1}$ number of score computations, which corresponds to an exact reduction by half. \square

A.5 Computational gains for arbitrary tiers

In this section we provide an extension of the above theorem to an arbitrary number of tiers with arbitrary sizes.

Theorem 9. *Given a set of full parent graphs, incorporating tiered domain knowledge that includes n tiers $\{\mathbf{T}_1, \dots, \mathbf{T}_n\}$ reduces the maximum number of score function computations in regular A^* -based causal discovery from $p2^{p-1}$ to the following:*

$$\sum_{k=1}^{n-1} |\mathbf{T}_k| 2^{p-1-\sum_{l=k+1}^n |\mathbf{T}_l|} + |\mathbf{T}_n| 2^{p-1}, \quad (10)$$

where $|\mathbf{T}_k|$ is the number of variables in tier k .

Proof. Consider the tier \mathbf{T}_k containing $|\mathbf{T}_k|$ variables, including the variable $x_i \in \mathbf{T}_k$. By the definition of tiered domain knowledge, any variable x_j that is a member of a later tier \mathbf{T}_l , i.e. $k < l$ cannot be a parent of x_i . The number of such variables x_j that cannot be parents of x_i is obtained by summing over the sizes of all subsequent tiers, i.e. $\sum_{l=k+1}^n |\mathbf{T}_l|$. The size of the parent graph for variable x_i is then $2^{p-1-\sum_{l=k+1}^n |\mathbf{T}_l|}$, where p are the total number of variables. Consequently, the total number of score function evaluations for tier \mathbf{T}_k is $|\mathbf{T}_k| 2^{p-1-\sum_{l=k+1}^n |\mathbf{T}_l|}$. This holds true for all $1 \leq k < n$, but not for the last tier \mathbf{T}_n , where no later tiers exist and the total number of score function evaluations remains $|\mathbf{T}_n| 2^{p-1}$. Note that elements in the first tier \mathbf{T}_1 no longer have empty parent graphs since edges between elements in the same tier are allowed. The total number of score function evaluations is then:

$$\sum_{k=1}^{n-1} |\mathbf{T}_k| 2^{p-1-\sum_{l=k+1}^n |\mathbf{T}_l|} + |\mathbf{T}_n| 2^{p-1}. \quad (11)$$

\square

A.6 Visualizing the parent graph pruning

In Figure 2 of the main text, we visualize parent graphs that have been pruned due to the insertion of domain knowledge, specifically that of known edges and forbidden edges. We here provide further visualizations of pruned parent graphs for all types of domain knowledge. Specifically, Figure 5 shows the pruned parent graphs of x_1 (left) and x_4 (right) when incorporating the known edge $x_4 \rightarrow x_1$, while Figure 6 shows the pruned parent graphs of x_1 (left) and x_4 (right) when incorporating a forbidden edge between them. Figure 7 shows the parent graphs of x_4 (left) and x_2 (right) when incorporating tiers such that x_1 is a source variable and x_4 is a sink variable.

B Additional experiment information

B.1 Evaluation

As mentioned in the main text, we evaluate the performance of all causal discovery methods by their ability to recover the true graph, as measured by the structural hamming distance (SHD) between *modified* CPDAGs. Recall that A^* -based methods return a *modified* CPDAG, where Meek's rules

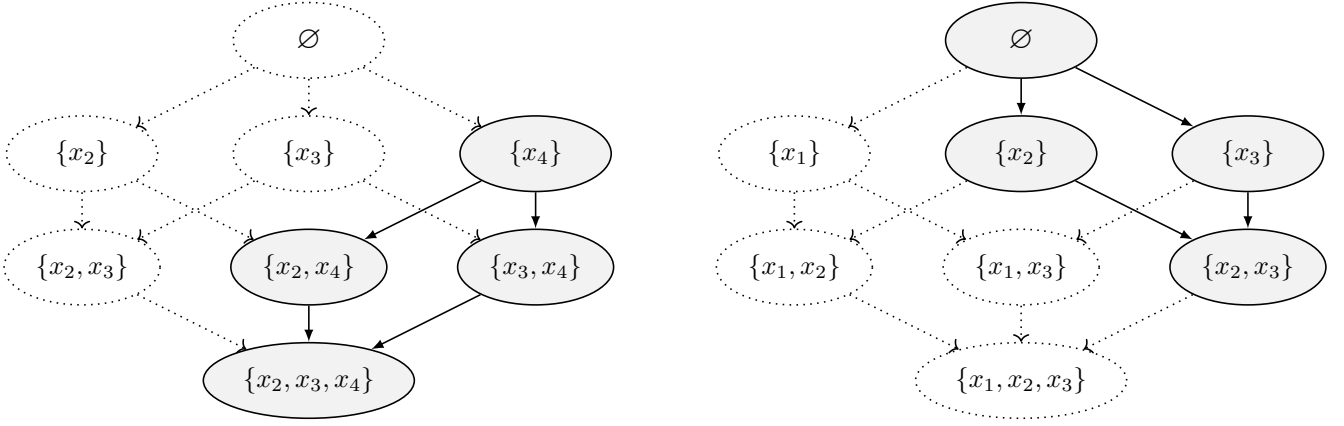


Figure 5: Pruned parent graphs $\mathcal{G}_{Pa}(x_1)$ (left) and $\mathcal{G}_{Pa}(x_4)$ (right) when incorporating a known edge $x_4 \rightarrow x_1$.

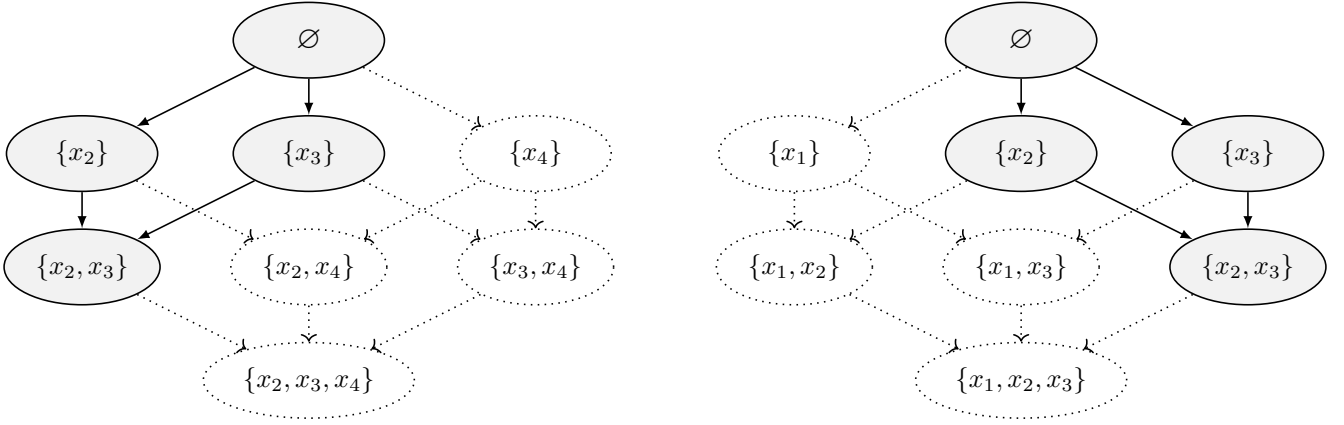


Figure 6: Pruned parent graphs $\mathcal{G}_{Pa}(x_1)$ (left) and $\mathcal{G}_{Pa}(x_4)$ (right) when incorporating a forbidden edge between x_1 and x_4 .

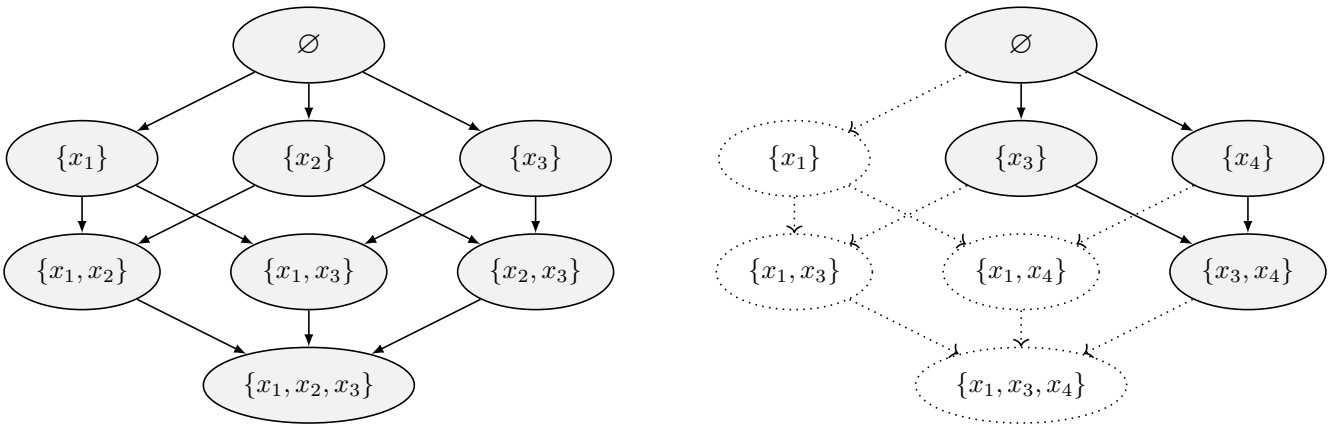


Figure 7: Pruned parent graphs when incorporating the tiers $\mathbf{T} = \{\{x_1\}, \{x_2, x_3\}, \{x_4\}\}$ such that x_1 is a source variable and x_4 is a sink variable. Shown are the parent graphs $\mathcal{G}_{Pa}(x_4)$ for the sink variable x_4 (left), which in fact does not change, and $\mathcal{G}_{Pa}(x_2)$ (right), which has the same number of nodes as the pruned parent graph $\mathcal{G}_{Pa}(x_3)$. Note that the pruned parent graph $\mathcal{G}_{Pa}(x_1)$ only contains the empty set.

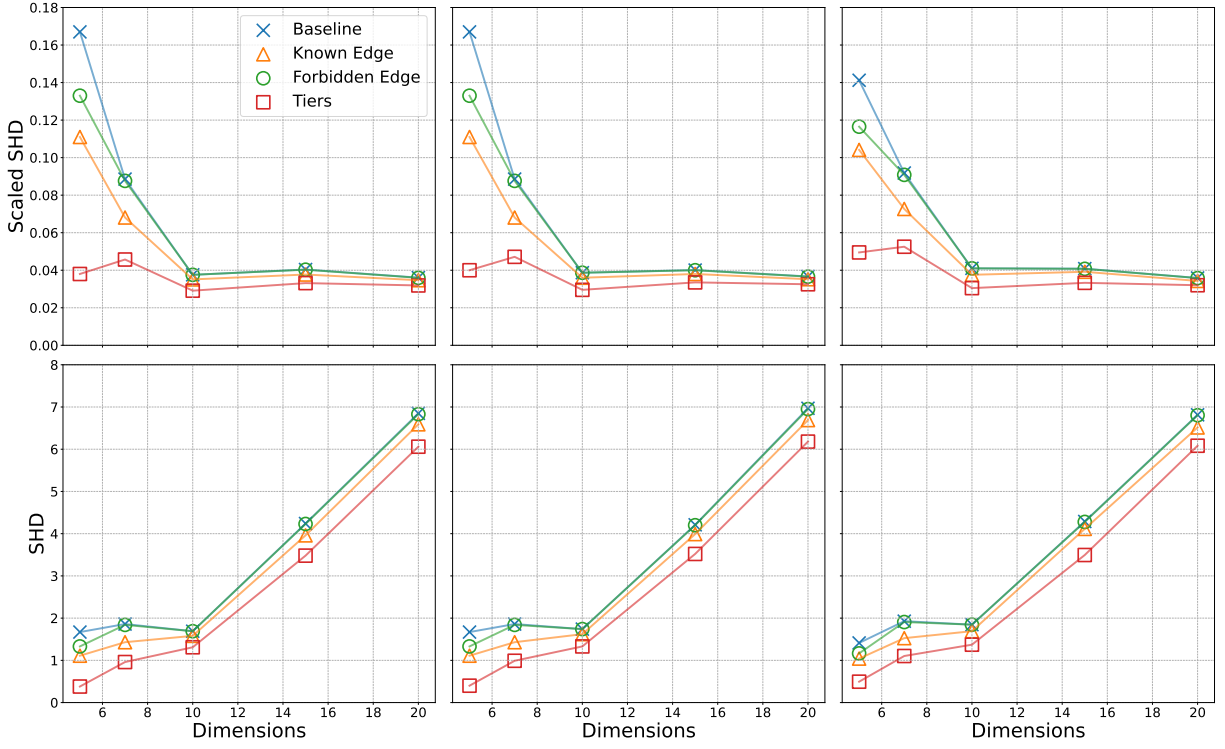


Figure 8: Scaled SHD (top row) and regular SHD (bottom row) for varying dimensions when applying regular A* (left column), A*-SuperStructure (middle column) and Local A* (right column) on the synthetic data set, averaged over 100 repeats.

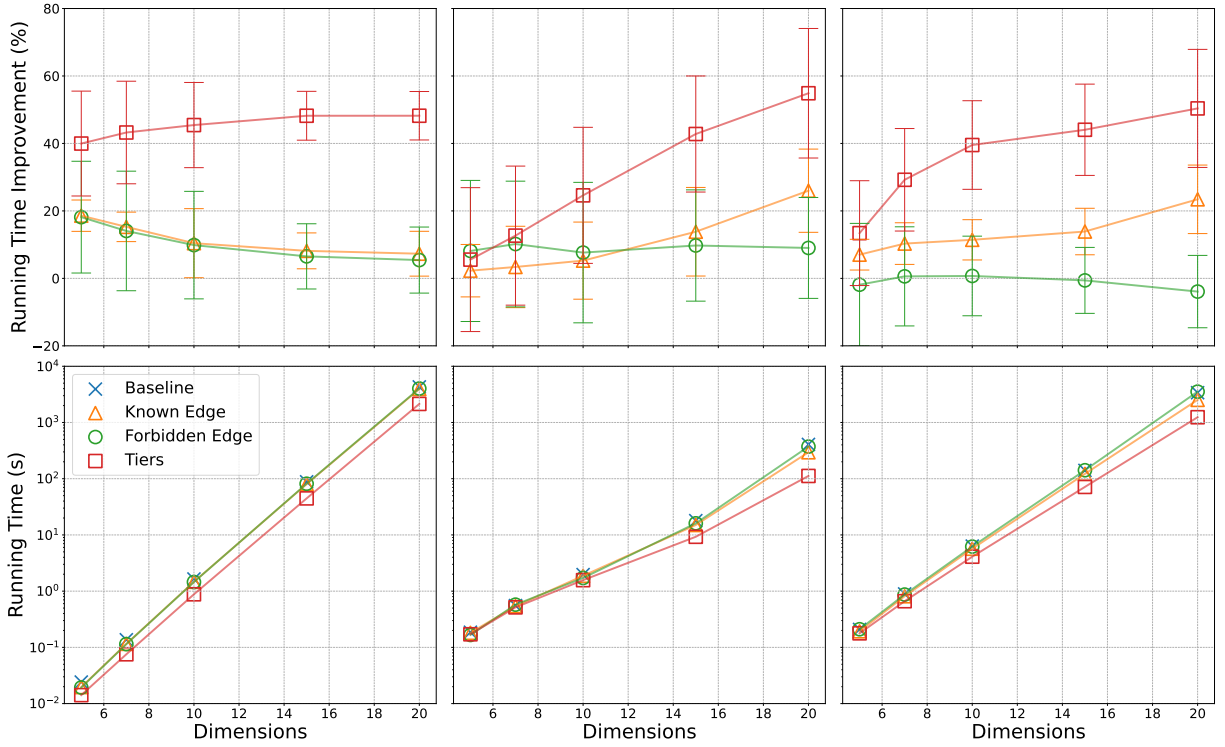


Figure 9: Percentage running time improvements (top row) and absolute running time (bottom row) for varying dimensions when applying regular A* (left column), A*-SuperStructure (middle column) and Local A* (right column) on the synthetic data set, averaged over 100 repeats. The error bars indicate one standard deviation from the mean.

have been applied post-discovery to ensure that the resulting CPDAG complies with the provided domain knowledge. To ensure a fair comparison, we therefore compute the CPDAG of the ground-truth DAG and then similarly apply Meek’s rules. This allows us to measure causal discovery performance via the SHD between the modified CPDAG estimate and the modified CPDAG of the ground-truth. We consider the SHD between different types of edges in a CPDAG to be 1 unless they are exactly the same, e.g. $\text{SHD}(\leftarrow, \rightarrow) = 1$, $\text{SHD}(\leftarrow, \dashv) = 1$ and $\text{SHD}(\leftarrow, \leftarrow) = 0$. Furthermore, in order to allow for a fair comparison of running times, all experiments were run on a single AMD Ryzen 7 3800X CPU.

B.2 Synthetic data

In our synthetic data experiments, we generate random ground-truth DAGs \mathcal{G} using the Erdős-Rényi algorithm, with an average degree of 2 and varying dimensions of $p \in \{5, 7, 10, 15, 20\}$. We then generate data by means of a linear structural equation model (SEM), i.e.

$$x_i = \sum_{j \in \text{Pa}_{\mathcal{G}}(x_i)} w_j x_j + \epsilon_i, \quad (12)$$

where $x_j \in \text{Pa}_{\mathcal{G}}(x_i)$ is a parent of x_i in \mathcal{G} . The linear weights w_j are randomly sampled from either $U(-0.2, -0.8)$ or $U(0.2, 0.8)$, chosen by a coin flip. The noise variables ϵ_i are sampled from a Gaussian distribution $\epsilon_i \sim \mathcal{N}(0, \sigma_i)$, where $\sigma_i \sim U(1, 2)$. For each random DAG \mathcal{G} we generate 500 observations using the same set of linear weights and noise standard deviations $\{\sigma_i\}_{i=1}^p$.

We here provide further experimental results that supplement those in the main text. Specifically, Figure 8 shows the scaled SHD (top row) and regular (SHD) for all types of domain knowledge, for all A*-based methods and for varying dimensions. The SHD improvements of A*-SuperStructure and Local A* are largely similar to those of regular A*, with Local A* performing slightly worse. Similarly, Figure 9 shows additional figures for computational running time improvements. The top row shows the percentage improvements including error bars, corresponding to one standard deviation. The behavior of Local A* is relatively similar to that of A*-SuperStructure. Notably, however, for Local A* the running times when integrating forbidden edges (shown in green) are worse than when not integrating any domain knowledge. The poor running time improvements when integrating forbidden edges with A*-SuperStructure and Local A*, as compared to integrating other types of domain knowledge, may be explained by the fact that graphical LASSO also prunes the parent graphs. Specifically, the pruning resulting from applying graphical LASSO has the same effect as integrating forbidden edges, since the resulting super-structure contains information about which edges might exist and, more importantly, which edges cannot exist. In this sense, integrating forbidden edges does not help with the running times of A*-SuperStructure and Local A* because graphical LASSO is likely to already have captured those forbidden edges as part of estimating the super-structure.

We note that all of our experiments were run on a single CPU and, unlike the other methods, Local A* has the poten-

tial to be parallelized over several CPUs (Ng et al. 2021), which means that it could potentially be faster when being parallelized. The construction of local clusters in Local A* (which would be the aspect to parallelize) carries some computational overhead, which would explain its poor performance on a single CPU core. The bottom row in Figure 9 shows corresponding absolute running times in seconds. A*-SuperStructure and Local A* tend to be slower than regular A* for small dimensions, presumably due to the computational overhead of the super-structure estimation, while they are faster for larger dimensions. A*-SuperStructure seems to have exceptional running time performance for large dimensions, as compared to the other methods.

Lastly, we present p-values from student’s t-tests with the null hypothesis that integrating known edges (Table 1), forbidden edges (Table 2) or tiers (Table 3) improves the SHD, as compared to not integrating any domain knowledge. Tables 1 and Table 3 show that we can be confident, with a p-value threshold of 0.05, that integrating known edges and tiers improves the SHD for nearly all dimensions. However, Table 2 shows that the same is not true for integrating forbidden edges, as we can only confidently say that this improves SHD for small, i.e. 5, dimensions.

B.3 Sachs data

In Figure 10 we visualize the ground-truth DAG corresponding to the real, protein signal-processing data set of Sachs et al. (2005). This ground-truth was formed using expert knowledge and, partly, interventional data. See Sachs et al. (2005) for more information.

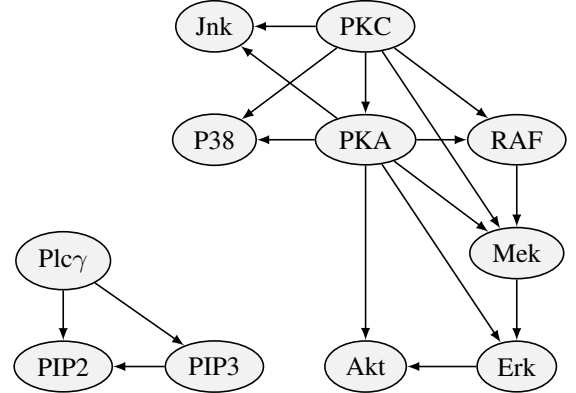


Figure 10: Ground-truth DAG for the real protein signalling dataset of Sachs et al. (2005), formed by experts using interventional data.

	Dimensions				
	5	7	10	15	20
A*	0.0001	0.0003	0.0020	0.0003	0.0001
A*-SuperStructure	0.0001	0.0003	0.0012	0.0017	0.0001
Local A*	0.0060	0.0004	0.0017	0.0614	0.0001

Table 1: P-values from a student’s t-test with the null hypothesis that integrating *known edges* improves SHD.

	Dimensions				
	5	7	10	15	20
A*	0.0144	0.2085	N/A	0.1599	0.0792
A*-SuperStructure	0.0144	0.2085	N/A	0.1599	0.0792
Local A*	0.0343	0.2085	N/A	0.1599	0.1599

Table 2: P-values from a student’s t-test with the null hypothesis that integrating *forbidden edges* improves SHD. N/A indicates that no student’s t-test could be performed because no run showed any SHD improvements.

	Dimensions				
	5	7	10	15	20
A*	0.0007×10^{-4}	0.0182×10^{-4}	6.8020×10^{-4}	0.7873×10^{-4}	0.0040×10^{-4}
A*-SuperStructure	0.0006×10^{-4}	0.0356×10^{-4}	3.8586×10^{-4}	0.7552×10^{-4}	0.0010×10^{-4}
Local A*	0.3255×10^{-4}	0.2331×10^{-4}	1.1118×10^{-4}	0.2188×10^{-4}	0.0007×10^{-4}

Table 3: P-values from a student’s t-test with the null hypothesis that integrating *tiers* improves SHD.